

PIXE ANALYSIS OF HAWAIIAN VOLCANICS: AN ANALOGUE FOR APXS IN GALE CRATER

J.A. Berger¹, M.E. Schmidt², R. Gellert¹, J.L. Campbell¹, E.L. Flannigan¹, R.V. Morris⁴, D.W. Ming⁴. ¹University of Guelph, Guelph, CAN, jberge01@uoguelph.ca; ²Brock University, St. Catharines, CAN; ³; ⁴NASA JSC, Houston, USA.

Introduction: Gale Crater sedimentary rocks have a mixed provenance and a range of alteration characteristics, as evident in geochemical trends found in basaltic and alkalic sedimentary rocks by *Curiosity's* Alpha Particle X-ray Spectrometer (APXS) [e.g., 1,2]. Parent sediment compositions are not well-constrained, which complicates interpretations of geochemical variations. Thus, we look to altered post-shield volcanics from Kohala and Maunakea (aka Mauna Kea) as a Martian analogue. The Hawaiian volcanics have compositions similar to Gale, and exhibit multiple alteration pathways, so they are useful to aid our interpretations of Gale Crater geochemical observations.

The rover-based APXS is a combination of Particle Induced X-ray Emission spectrometry (PIXE) and X-ray Fluorescence spectrometry (XRF) [3]. Using laboratory XRF as an analogue for APXS on Mars is convenient because XRF is an accurate, standard geochemical method. However, differences in sample preparation and the physics of sample interrogation can lead to different results for XRF and APXS of the same material. We thus evaluate broad beam PIXE here as an APXS analogue.

Methods: 43 samples of unaltered and altered lava and tephra from Kohala and Maunakea were analyzed by PIXE. Pedogenic alteration profiles were obtained at roadcuts below 9000 m elevation. Palagonitic and acid sulfate altered tephra were collected at the Maunakea summit. Parent compositions cover the full range of the post-shield volcanics from basalt to alkalic hawaiite-mugearite-benmoreite.

PIXE samples were analyzed as pressed powder pellets, which is a method similar to the APXS calibration dataset [3]. Samples were milled in an aluminum ball mill for 8-20 min. to a ~20 μm mean grain size and pressed into 13 mm diameter pellets without additives. PIXE analyses were conducted at the University of Guelph according to the method of [4] with a 4 mm x 4 mm, 2.5 MeV proton beam. Counting times (~3 min.) were determined by the integrated beam charge of 10 μC , and counts per second were maintained at ~1200-2300 with a beam current of ~8.5-12 nA.

Determination of elemental concentrations was completed with the PIXE spectrum fitting software package GUPIX [5]. The software uses a nonlinear least-squares fitting algorithm and converts peak areas to elemental concentrations by standardization based on fundamental parameters. Samples are treated as 'unknown', thus the matrix is calculated iteratively so that matrix attenuation and secondary fluorescence can be

determined. An infinitely thick sample that is homogeneous on the sub- μm scale is assumed.

The assumption of homogeneity is problematic for broad beam PIXE (as well as XRF, APXS) of powdered geologic samples because the matrix is not homogeneous on the sub- μm scale [4]. We employed an empirical correction to account for the systematic offset of concentrations due to these matrix effects. The correction factors were determined by analyzing splits of 24 of the 43 samples with standard XRF (at WSU) of *fused glass beads* to minimize matrix effects. These were used as standard concentrations, and the mean PIXE/XRF (R-value) for each element was used as a correction, with ± 1 standard deviation taken as the error in accuracy.

Sulfur accuracy was evaluated differently, using PIXE analyses of mixtures of Maunakea basalt with known amounts of pure K_2SO_4 . Work is preliminary and SO_3 corrections were not determined.

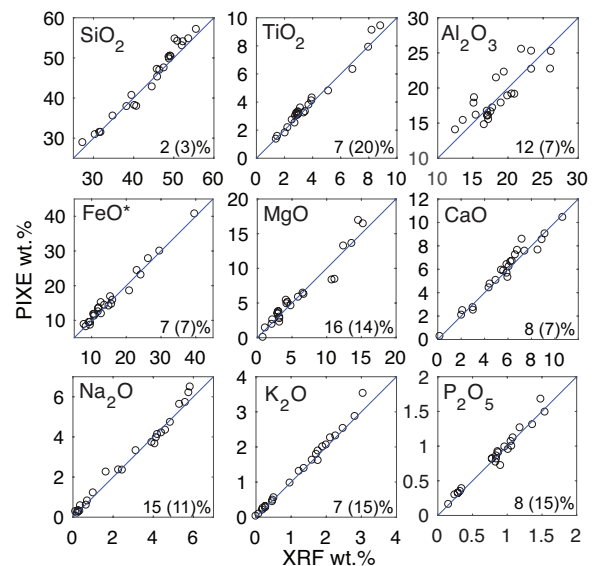


Fig. 1: Corrected PIXE concentrations versus XRF concentrations for Maunakea calibration samples, renormalized to volatile-free concentrations. Relative % error in PIXE accuracy is shown, with APXS error in parentheses [3]. Lines indicate the 1:1 slope though the origin.

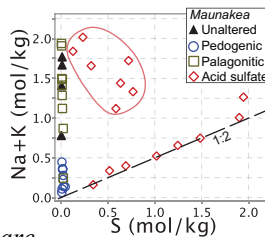
Results: Fig. 1 presents the results for the 24 standards used to determine R-values and accuracy. The largest PIXE errors are found in Na_2O , MgO , and Al_2O_3 , because they are the lightest elements and subject to the greatest matrix effects. For example, the attenuation of

Al_2O_3 by FeO is overestimated in olivine-phyric samples because the Al in feldspar is not intimately mixed with the Fe in olivine on the sub- μm scale.

Sulfur accuracy for pure K_2SO_4 is high, but R-values (and error) increase systematically with decreasing K_2SO_4 concentrations in a basalt matrix. This is again a heterogeneous matrix effect: the attenuation of S by Si is overestimated as Si increases in the matrix. The relative error for SO_3 at concentrations below 10 wt% is ~20-30%, which is comparable to APXS [3]. We find, however, that the SO_3 results are consistent with the samples and precision is high (Fig. 2).

The PIXE error is similar overall to APXS (Fig. 1). Nine olivine-phyric samples caused the Al_2O_3 error to be larger for PIXE. The accuracy errors of TiO_2 , K_2O , and P_2O_5 are higher for APXS because they have different background considerations [3].

Fig. 2: Maunakea PIXE results showing molar Na+K versus S. The line indicates the molar variation of 1:2 (Na+K):S by addition of K- and Na-bearing alunite group sulfates. The S-bearing samples with high Na+K (polygon) are breccias of hawaiiite and sulfate, whereas the samples near the line are primarily sulfates with highly altered hawaiiite.



Comparison of Hawai'i to Gale Crater:

The altered Hawaiian volcanics studied here are relevant to the apparently altered rocks of the Mt. Sharp Group up to the Vera Rubin Ridge (sols 700-1795). Excepting light-toned, fracture-associated haloes, the unaltered parent composition(s) (i.e., provenance) is (are) unknown. We therefore assume soil (avg. Mars) represents a plausible parent composition to approximate element trends. We use Ti for element ratios here because it is generally immobile over a wide pH range. Overall, Mt. Sharp alteration is characterized by silica enrichment and divalent cation depletion relative to soil. Three trends are notable:

(1) Si/Ti: In the Hawaiian samples, TiO_2 is passively enriched with silica in residue via acid sulfate alteration, resulting in a small increase in Si/Ti (Fig. 3a). Open-system hydrolysis leads to silica leaching and enrichment of TiO_2 in pedogenic and palagonitic residue, thus decreasing Si/Ti. Silica enrichment at Mt. Sharp corresponds with no change, or a small increase, in Si/Ti, consistent with passive enrichment of the two elements (Fig. 3d).

(2) K/Ti: At Hawai'i, incipient pedogenic alteration leaches alkali elements, and extensive weathering results in removal of nearly all K_2O . In contrast, acid sulfate alteration retains mobile K in alunite group sulfates

(Figs. 2b, 3b). K_2O is elevated in the Murray fm. (Fig. 3e), suggesting K was added and/or retained.

(3) P/Ti: In the Hawaiian samples, absolute P_2O_5 concentrations typically do not change with open-system pedogenic alteration, but small decreases in P/Ti indicates limited P mobility (Fig. 3c). With acid sulfate alteration, P_2O_5 and P/Ti increase. Primary apatite likely dissolves in the acid sulfate system, forming insoluble Fe-phosphates. Mt. Sharp bedrock has variable P_2O_5 , including several strongly enriched diagenetic targets (Fig. 3f), indicating that the element was mobile.

Conclusion: Broad beam PIXE replicates the response and accuracy of APXS relatively well, and is a promising analogue lab technique. Acid sulfate alteration trends in the Hawaiian rocks are consistent with the SiO_2 , TiO_2 , K_2O , and P_2O_5 enrichments found in Mt. Sharp bedrock and haloes; Gale units do not have the characteristics of the residue of pedogenic, open system weathering common on Hawai'i.

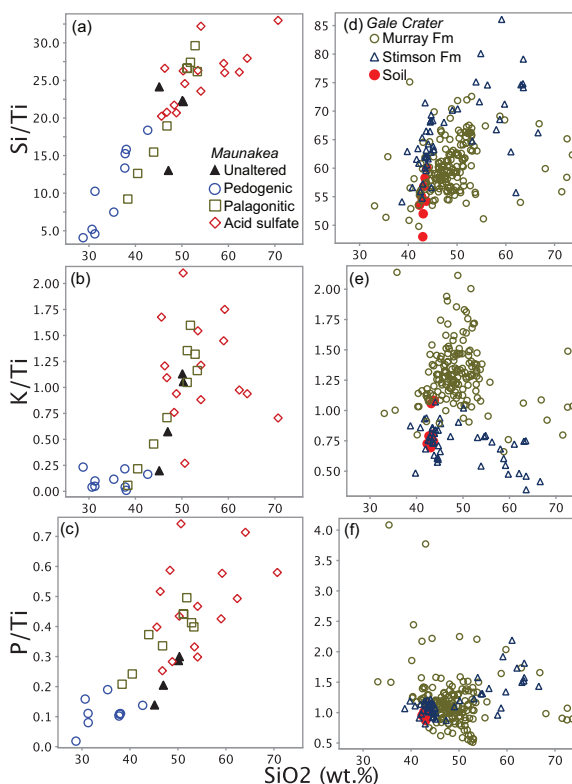


Fig. 3: Ti-normalized element trends at (a-c) Maunakea (PIXE) and (d-f) Gale Crater (APXS; without Ca-sulfate-rich targets).

Acknowledgements: This research was funded in part by the Canadian Space Agency through a PS grant to M.E.S.

References: [1] Thompson et al. (2016) JGR-Planets. [2] Berger et al. (2017) JGR-Planets. [3] Gellert et al. (2006) JGR-Planets. [4] Flannigan and Campbell (2017) Nucl. Instrum. Methods Phys. Res.B. [5] Campbell et al., (2010) Nucl. Instrum. Methods Phys. Res.B.